Can we Execute Reliable MM-PBSA Free Energy Computations of Relative Energies of Different Guanine Quadruplex Folds?

***Barira Islam*[†], *Petr Stadlbauer*[†], *Stephen Neidle*[§], *Shozeb Haider*[§] *and Jiri Sponer*[† ‡ *]**

[†]Institute of Biophysics, Academy of Sciences of the Czech Republic, Královopolská 135, 612 65 Brno, Czech Republic

[§]UCL School of Pharmacy, 29-39 Brunswick Square, London WC1N 1AX, UK

[‡]CEITEC - Central European Institute of Technology, Masaryk University, Campus Bohunice, Kamenice 5, 625 00 Brno, Czech Republic

*Corresponding Author

Equilibration protocol. The solvated system was first minimized (500 cycles of steepest descent cycles followed by 500 cycles of conjugate gradient cycles) with a restraint of 25 kcal mol^{-1} $Å^{-2}$ on the solute (including the channel cations). Minimization with 5 kcal mol^{-1} $Å^{-2}$ restraints followed, using 500 steps of steepest descent method and 500 steps of conjugate gradient. The restraints of 5 kcal mol^{-1} $Å^{-2}$ were maintained on solute and the system was equilibrated for 50 ps at constant temperature of 300 K and pressure of 1 atm. An analogous series of alternating minimizations and equilibrations followed using decreasing position restraints of 4, 3, 2 and 1 kcal mol^{-1} $Å^{-2}$ consecutively. The final equilibration was carried out with position restraints of 0.5 kcal mol^{-1} $Å^{-2}$ and starting velocities from the previous equilibration, followed by a short free molecular dynamics simulation of 50 ps. Temperature and pressure coupling during equilibration was set to 0.2 and coupling during the last molecular dynamics phase was set to 5.

Free energy calculations based on simulations of GSs of models 0-7. The RMSD variations of the GSs in the simulations without the loops showed slightly different trends from RMSDs in equivalent simulations of full GQs (Figures S7-S9). Contrary to the simulations with the loops, GS **5** displayed stable RMSD in the simulations without the loops in all the three force-fields. This further supported our justification that significantly higher RMSD values of model **5** in simulations of full GQs were due to stem-loop interactions as discussed in the Main text (Figures 8, S5 and S6). The RMSD values of GS **3** were unstable in bsc0 force-field (Figure S7). Similarly, the RMSD values of GS **4** and GS **6** were unstable in the bsc0χ_{OL4} force-field (Figure S8). The significant fluctuations in RMSD values of GS **3**, GS **4** and GS **6** reflected instabilities of these GSs in the simulations. The instabilities were further confirmed by visualization of trajectories as strand slippage was observed within few ns of the start of these simulations. In the simulations of GS **3** in bsc0 force-field, the first guanine moved towards the bulk at 37 ns and then stacked over on the 5'-base of strand 3 at ~97 ns. In the simulations of GS **4** and GS **6** in

bsc0χ_{OL4} force-field, strand slippage was observed in the strand 4. For these geometries, we repeated the simulations with random seeds but could not achieve stable trajectories even after several attempts. It should be noted that, because the simulations correspond to non-native (experimentally unobserved) *syn-anti* GS patterns, the simulation behavior can be correct, though it may also indicate strain in the modeled starting structures.

It is noteworthy that in the simulations of the GSs from the models not all the 5'-*syn* bases could form the 5'-OH - (G)N3 H-bond (Table S8). For example, GS **1** and GS **7** have *syn* bases at the 5'-ends of all the four strands. The 5'-OH - (G)N3 H-bonds were formed only in the strands 2 and 4 and could not be formed in the strands 1 and 3 in all the force-fields. Thus, while the GSs extracted from experimental topologies always sampled the 5'-OH - (G)N3 H-bonds in all the strands with 5'-terminal *syn* throughout the simulations in all the force-fields, the the built-up models were not always capable to form them. It shows that the modeled starting structures are likely strained.

The MM-PBSA free energy results of model GSs are presented in the Tables S8 and S9. The energy of GS **5** was more converged than in the simulations with the loops. It showed a relative free energy of 3, 2 and -5 kcal/mol in the bsc0, bsc0χ_{OL4} and bsc0$\chi_{OL4}\varepsilon\zeta_{OL1}$ simulations, respectively. GS **5** has 5'-*syn* in two strands and its base-steps are equivalent to GS **0**. However, in the simulations of GS **5**, the intramolecular hydrogen bond was formed only in strand 1 (Table S8).

The GS **2** and GS **4** have 5'-*syn* in two out of four strands and have equivalent base-steps. In the simulations, while both the strands of GS **2** sampled the intramolecular hydrogen bonds, these bonds were not formed in GS **4**. Therefore, the predicted energy of GS **4** (by Cang *et al.* [34] data) is higher than that of GS **2**. GS **4** was highly structurally unstable in simulations in all three force-fields. In the simulations of GS **4**, *anti-syn* transitions were observed in first base of strand

4 in the bsc0 and bsc0$\chi_{OL4}\varepsilon\zeta_{OL1}$ force-fields and strand slippage was observed in the strand in bsc0χ_{OL4} force-field. GS **3** and GS **6** are predicted to have highest energy among the models using Cang *et al.*'s prediction. In agreement with this, the two model GSs showed higher energy than the other model GSs in the present MM-PBSA calculations (Table S8). GS **3** showed movement of 5'- guanine from the first strand towards the bulk in the bsc0 force-field. It had relative free energy of 23 and 15 kcal/mol in the more stable bsc0χ_{OL4} and bsc0$\chi_{OL4}\varepsilon\zeta_{OL1}$ force-fields, respectively. GS **6** also showed high relative free energy in all the three force-fields. Thus, despite that the GSs of the models showed large fluctuations in the energy values in many simulations due to visible structural perturbations; we still suggest that the trend of relative free energy is in agreement with the predictions from Cang *et al.*[34] (Table S8). It can be documented in the following way. For example, we can compare the models **0**, **3** and **6** from the above simulations. The models **0**, **3** and **6** have the equal numbers of AS steps (4 steps out of 8). The other 4 base-steps are SA in model **0** while they are SS (2 out of 8) and AA (2 out of 8) in models **3** and **6**. According to Cang *et al.*'s prediction, the SA step is more stabilizing than the other base-steps in the GQ. In the present MM-PBSA calculations as well, model **0** with 4 SA steps has lower energy than the models **3** and **6** with 2 AA and 2 SS steps. The higher energy of models **3** and **6** may be also related to the propensity of these GSs to develop instabilities in the simulations.

Another consistent result is that the energy contribution from 4 AS steps is more than from 2 SS and 2 AA steps. The 5'-*ssa--saa--saa--ssa*-3' (Htel topology antiparallel (2+2)) GS, 5'-*ssa--saa--ssa--saa*-3' (model **1**) GS and 5'-*saa--ssa--saa--ssa*-3' (model **7**) GS are more stable than 5'-*asa--sas--asa--sas*-3' (model **0**) GS in nearly all the simulations (Tables 2 and S6). The antiparallel (2+2), model **1** and model **7** have 4 SA, 2 SS and 2 AA steps while the model **0** (antiparallel basket) has 4 SA and 4 AS steps. If we take a mean of relative free energy of these GSs with respect to model **0** GS (-6 kcal/mol) and assume AA (0 kcal/mol) and AS (3.5

kcal/mol) contribution from Cang *et al.*[34] to be true, SS base-step energy estimate is +4 kcal/mol which is very close (considering the noise of the method) to the predicted energy of +4.6 kcal/mol. Thus, although, the energies in the three quartet system were more sensitive to minor structural perturbations, the trend of base-step stability is in agreement with the previous predictions based on two-quartet system.[34] This analysis considered only the bsc0 simulations since bsc0 has been used by Cang *et al.* Note, that for a direct comparison with experimental observations, the data by Cang *et al.* have to be corrected by the QM computations,[35] as described in the main text. The MM-GBSA values of the model GQs in simulations both with and without the loops also displayed similar trends (Table S10).

Legend to Supplementary Movie S1. The ion dynamics in Htel parallel-stranded GQ in the simulation carried out in the presence of 0.15 M excess NaCl in bsc0$\chi_{OL4}\varepsilon\zeta_{OL1}$ force-field. The GQ is shown in cartoon representation. The backbone of full GQ is shown in cyan. The stem nucleosides are shown in grey and loop nucleosides are not shown. The ions between the quartets are shown as purple and red spheres and the incoming bulk ion is shown as yellow sphere.

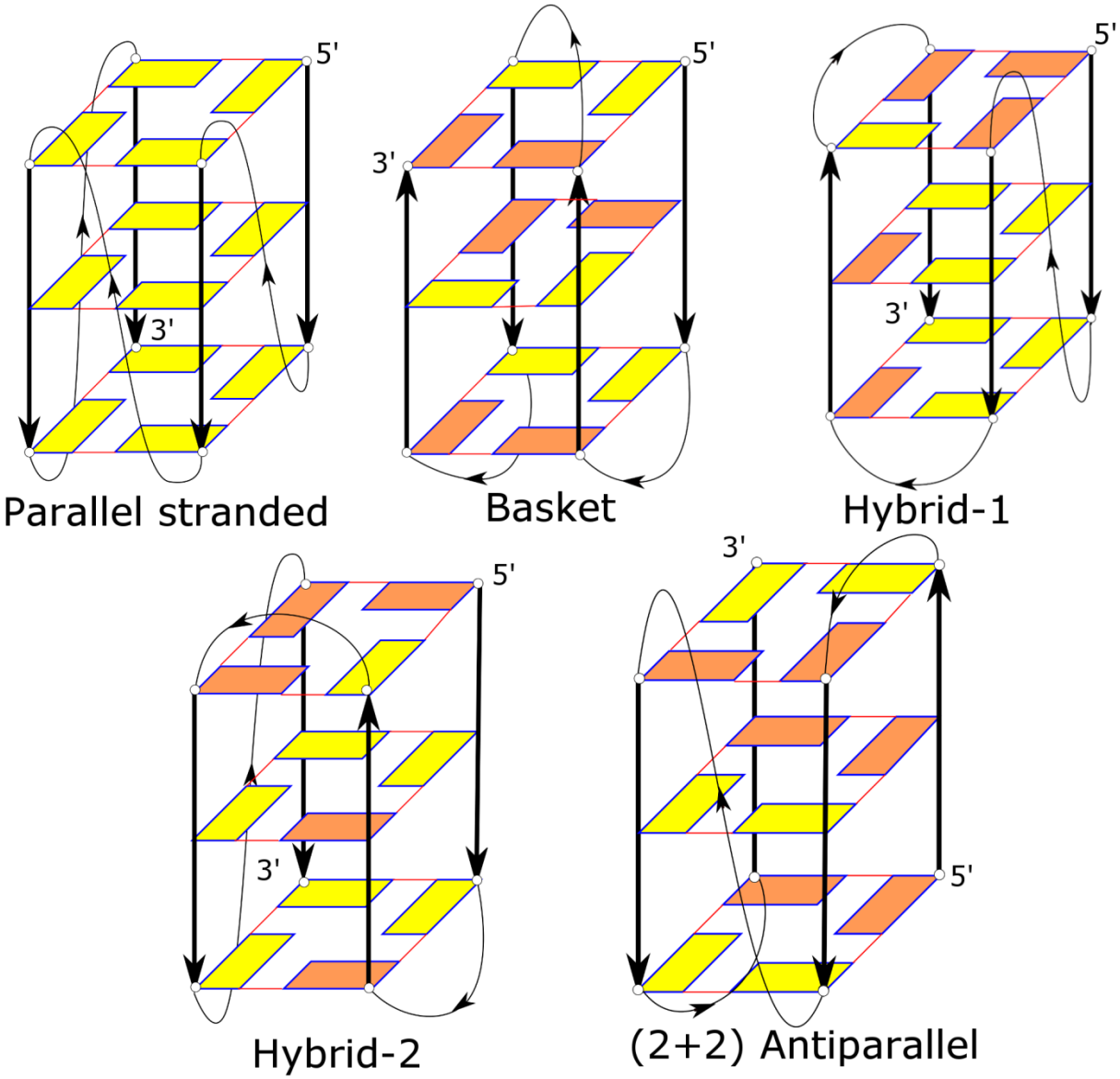

Figure S1. Schematic representation of intramolecular Htel GQ topologies used in the present study. The bases in *anti* and *syn* orientations are shown in yellow and orange, respectively.

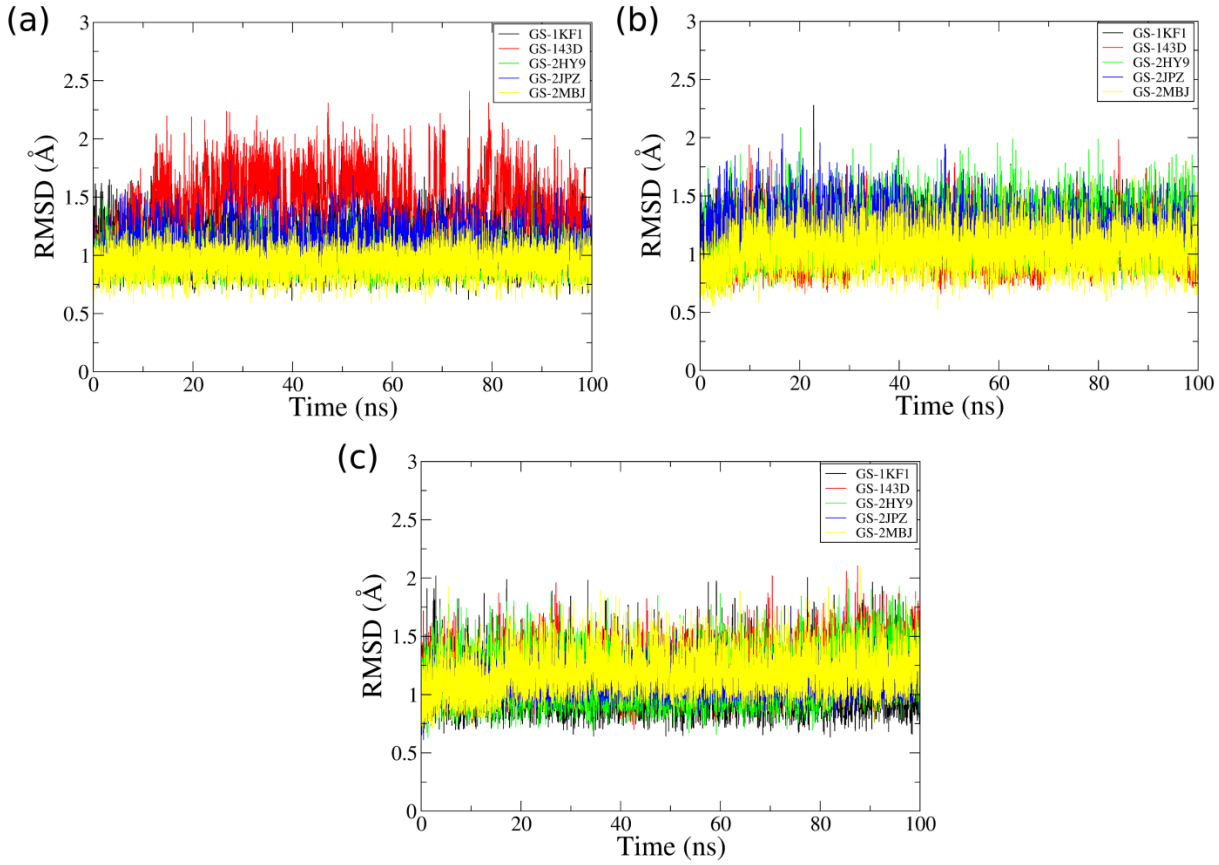

Figure S2. All atom mass-weighted RMSD vs. time curves for the Htel GSs simulated in (a) bsc0, (b) bsc0χ_{OL4} and (c) bsc0$\chi_{OL4}\varepsilon\zeta_{OL1}$ force-fields. The parallel-stranded (GS-1KF1), antiparallel basket (GS-143D), hybrid-1 (GS-2HY9), hybrid-2 (GS-2JPZ) and antiparallel (2+2) (GS-2MBJ) data are represented in black, red, green, blue and yellow. The simulations and MM-PBSA calculations were carried out only with the GSs.

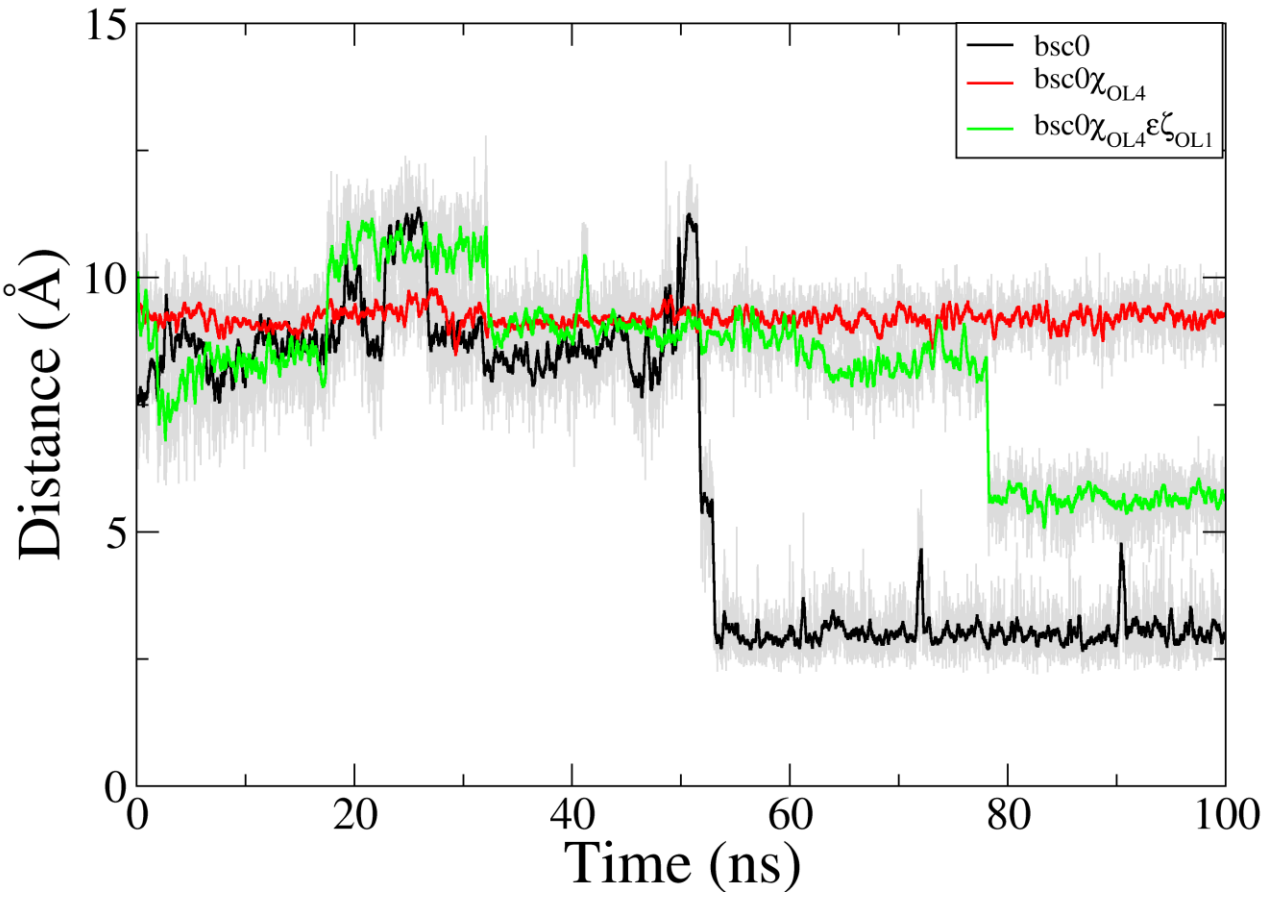

Figure S3. Distance vs. time plot showing the stem-loop interaction between A13(H2) and G14(O6) of antiparallel basket GQ. Stable hydrogen bond was formed in bsc0 force-field that eventually led to compaction of the narrow groove. The grey lines represent the snapshots while the black, red and green lines represent running averages over 250 ps.

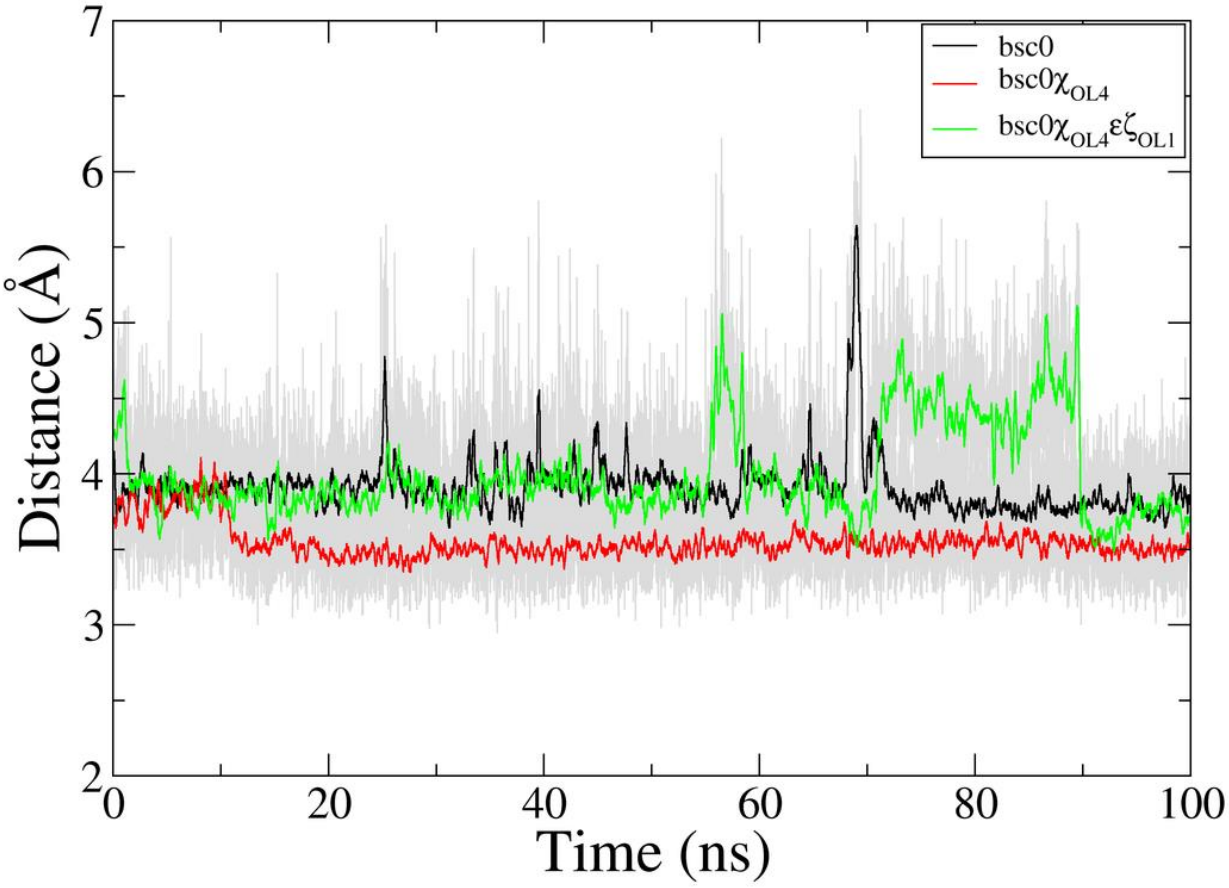

Figure S4. Inter-cationic distance vs. time plot in the simulations of full GQ of hybrid-2 topology in the bsc0, bsc0χ_{OL4} and bsc0$\chi_{OL4}\varepsilon\zeta_{OL1}$ force-fields. The grey lines represent the snapshots while the colored lines represent running averages over 250 ps.

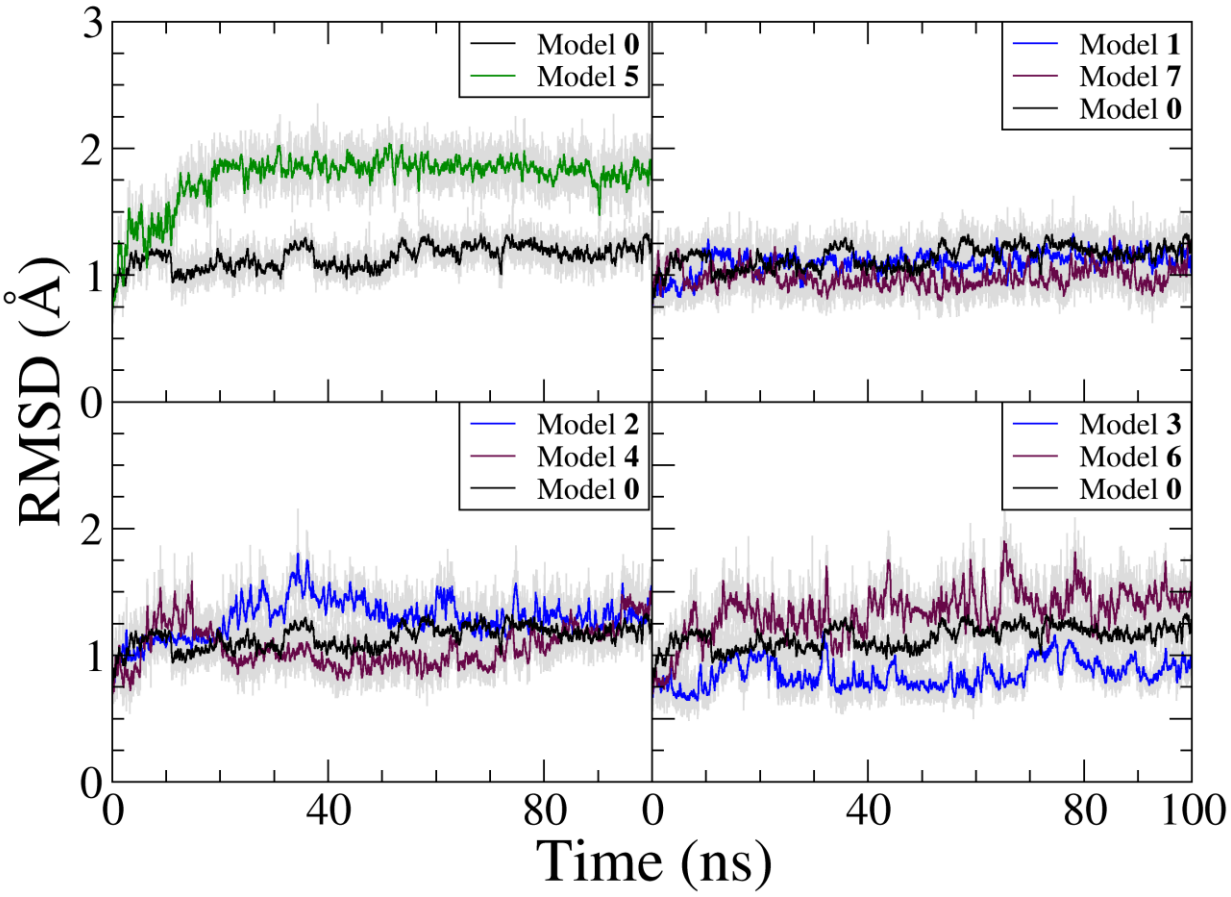

Figure S5. All atom mass-weighted RMSD vs. time curves for GSs of models **0 – 7** in the simulations carried with the full GQs in the bsc0 force-field. The grey lines in all the graphs represent the snapshots while the colored lines show the running averages over 250 ps. The models with identical base-steps are grouped together in the sub-plots.

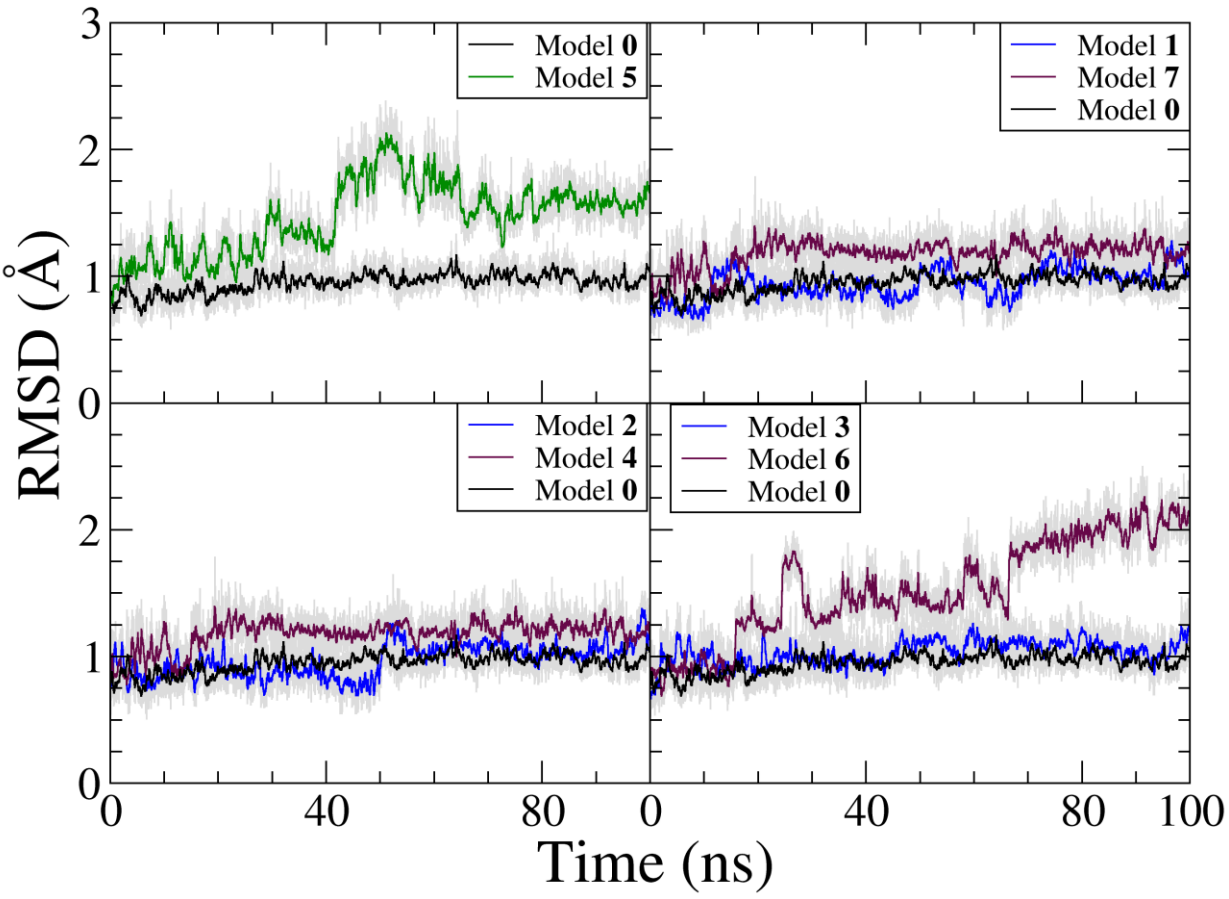

Figure S6. All atom mass-weighted RMSD vs. time curves for GSs of models in the simulations carried with the full GQ models in bsc0χ_{OL4} force-field. The grey lines in the graphs represent the snapshots while the colored lines show the running averages over 250 ps. The models with identical base-steps are grouped together in the sub-plots.

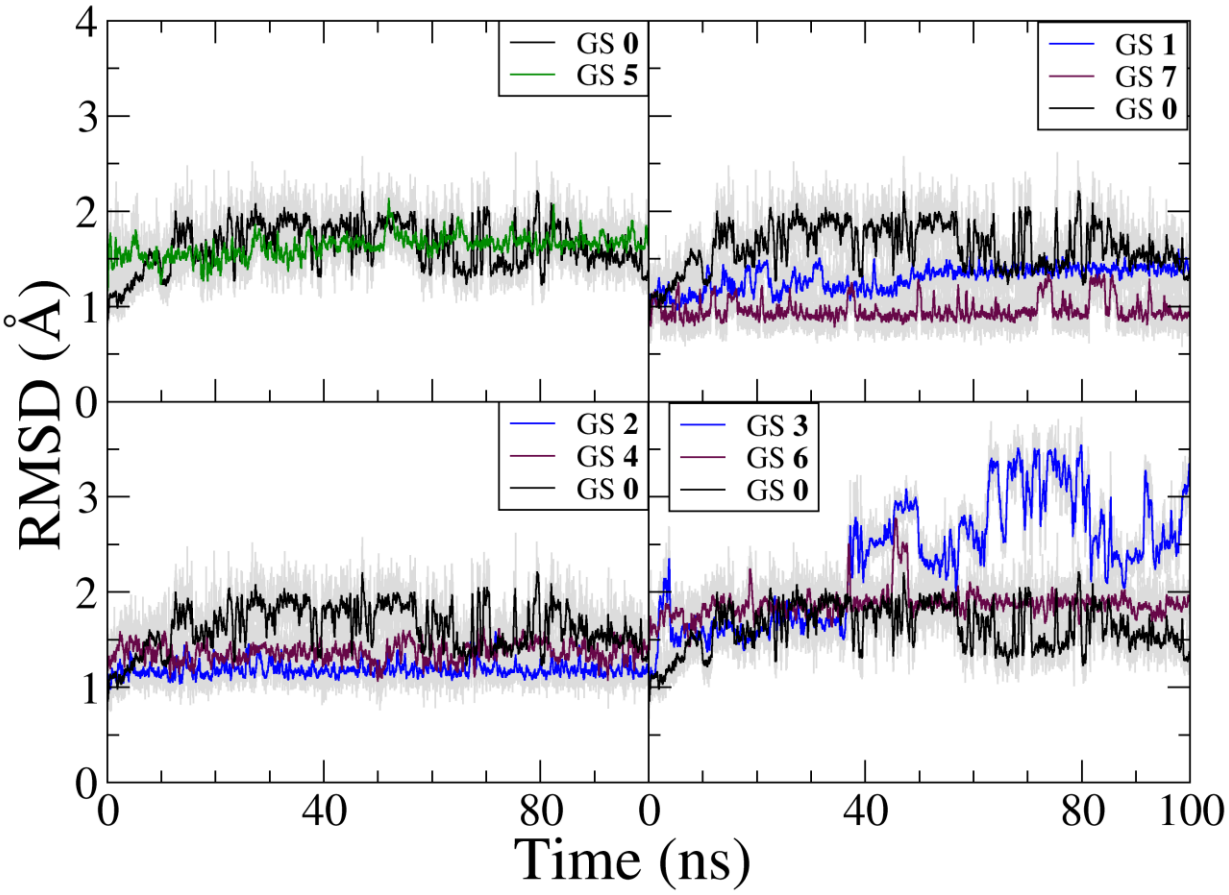

Figure S7. All atom mass-weighted RMSD vs. time curves for the GSs of the models in the bsc0 force-field. The simulations were carried out with only the GSs. The grey lines in the graphs represent the snapshots while the colored lines show the running averages over 250 ps. The GSs with identical base-steps are grouped together in the sub-plots.

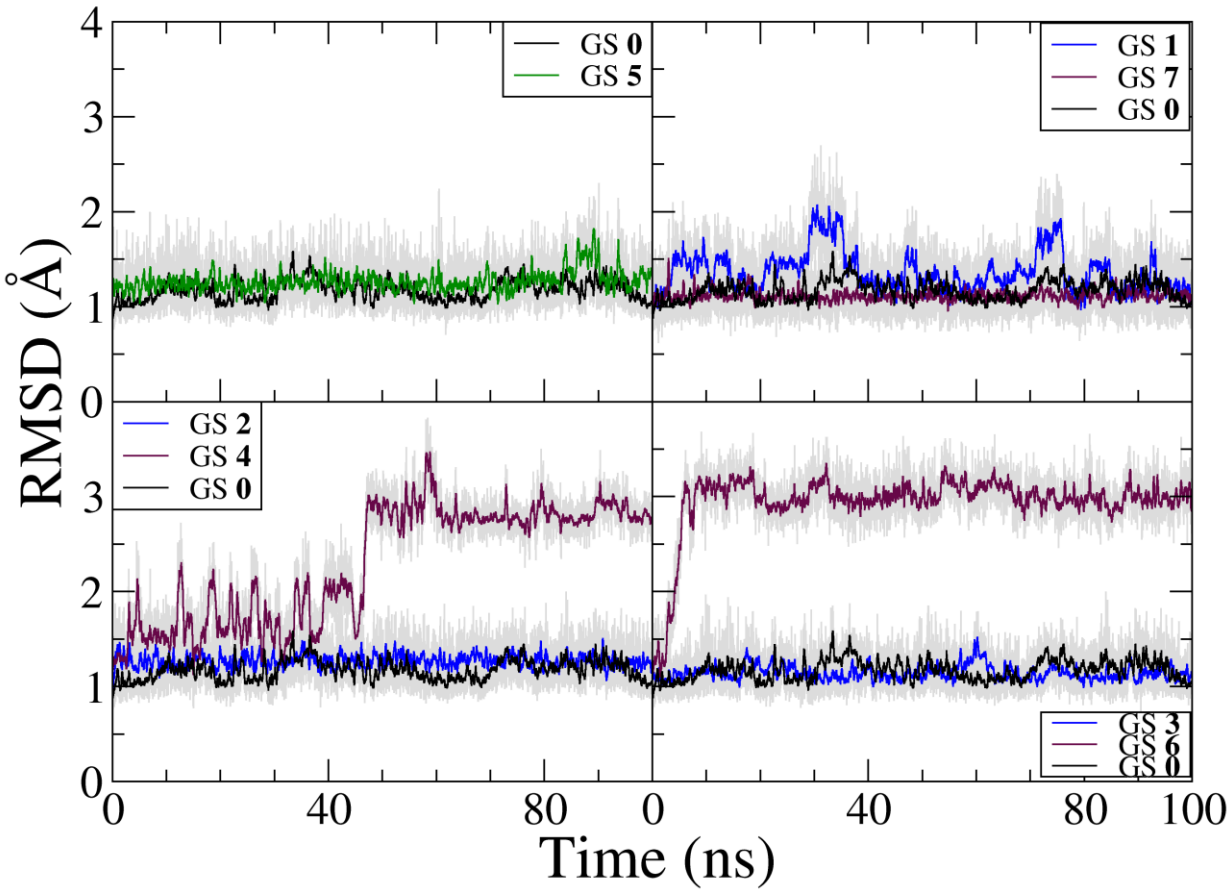

Figure S8. All atom mass-weighted RMSD vs. time curves for the GSs of the models in the bsc0χ_{OL4} force-field. The simulations were carried out with only the GSs. The grey lines in the graphs represent the snapshots while the colored lines show the running averages over 250 ps. The GSs with identical base-steps are grouped together in the sub-plots.

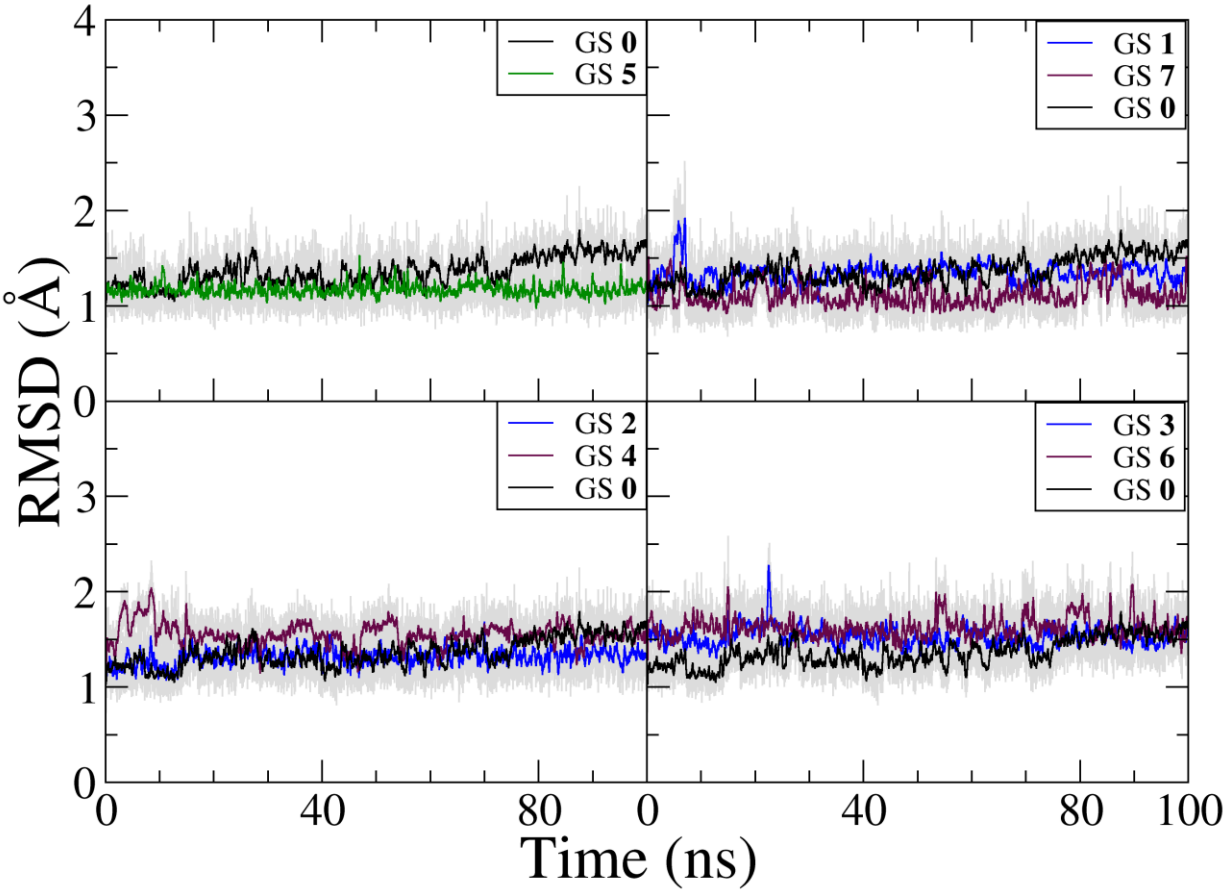

Figure S9. All atom mass-weighted RMSD vs. time curves for the GSs of the models in the bsc0$\chi_{OL4}\varepsilon\zeta_{OL1}$ force-field. The simulations were carried out with only the GSs. The grey lines in the graphs represent the snapshots while the colored lines show the running averages over 250 ps. The GSs with identical base-steps are grouped together in the sub-plots.

Table S1. Summary of loop interactions and alignments involving flanking bases and loops formed in the Htel full GQ simulations[a]

Topology	**bsc0**		**bsc0χ_{OL4}**		**bsc0$\chi_{OL4}\varepsilon\zeta_{OL1}$**	
	Time period used for MM-PBSA (ns)	**Remark about structures seen in the simulation**	**Time period used for MM-PBSA (ns)**	**Remark about structures seen in the simulation**	**Time period used for MM-PBSA (ns)**	**Remark about structures seen in the simulation**
Parallel-stranded	50-100	Above: nil Groove: GS-L in the grooves 1,2 and 3 Below: nil	50-100	Above: nil Groove: GS-L in the grooves 1,2 and 3 Below: nil	50-100	Above: nil Groove: GS-L in the grooves 1,2 and 3 Below: nil
Anti-parallel basket	50-100	Above: S, GS-L Groove: nil Below: T	50-100	Above: BP Groove: nil Below: BP	50-100	Above: BP Groove: nil Below: BP
Hybrid-1	50-100	Above: S Groove : GS-L in the groove 1 Below: T	50-100	Above: S Groove: GS-L in groove 1 Below: BP	50-100	Above: S, BP Groove: GS-L in the groove 1 Below: T
Hybrid-2	50-100	Above: T, S Groove: GS-L in the groove 3 Below: T	50-100	Above: T, S Groove: GS-L in groove 3 Below: BP	50-100	Above: T, S Groove: GS-L in the groove 3 Below: BP, S
Anti-parallel (2+2)	50-100	Above: T Groove: GS-L Below: two T	50-100	Above-T Groove: GS-L Below: T, BP	50-100	Above-T Groove: GS-L Below: T, S

[a] The loops can align above the first quartet, below the third quartet and can interact in the grooves of the GQ. These interactions in the simulations of GQ topologies are summarized in the above table. A number is specified when more than one interaction/alignment is formed, which is particularly relevant for the grooves. The loops can interact with the GSs to form stable hydrogen bonds (GS-L). Three or more flanking and/or loop nucleotides can stack over one another (S) to form ladder like structure. The flanking and/or loop nucleotides can form hydrogen bonds and align to form triad (T) or base-pair (BP).

Table S2. MM-PBSA-based free energies[a] (kcal/mol) of the Htel topologies[b]

Topology	MM_ele	MM_vdw	MM_int	PB_sur	E_disp	PB_cal	*G*	Δ*G*
bsc0								
Parallel-stranded	-1461	-106	559	27	-258	-1894	-3133	0
Antiparallel basket	-1318	-105	548	27	-250	-2014	-3112	21
Hybrid-1	-1399	-110	560	27	-249	-1942	-3113	20
Hybrid-2	-1390	-107	558	27	-253	-1957	-3122	11
Antiparallel (2+2)	-1349	-105	545	27	-248	-1998	-3128	5
bsc0χ_{OL4}								
Parallel-stranded	-1472	-102	562	27	-258	-1888	-3131	0
Antiparallel basket	-1364	-103	553	27	-251	-1978	-3116	15
Hybrid-1	-1417	-103	561	27	-250	-1931	-3113	18
Hybrid-2	-1408	-103	562	27	-252	-1934	-3108	23
Antiparallel (2+2)	-1338	-106	543	27	-248	-2001	-3123	8
bsc0$\chi_{OL4}\varepsilon\zeta_{OL1}$								
Parallel-stranded	-1472	-101	563	27	-258	-1887	-3128	0
Antiparallel basket	-1340	-104	548	27	-250	-1996	-3115	13
Hybrid-1	-1391	-106	559	27	-247	-1951	-3109	19
Hybrid-2	-1407	-104	559	27	-250	-1937	-3112	16
Antiparallel (2+2)	-1358	-106	548	27	-248	-1987	-3124	4

[a] The MM_ele, MM_vdw and MM_int represent the electrostatic, van der Waals and the internal (bond, angle and dihedral angle) potential energies. The PB_sur and PB_cal represent non-polar cavitation and polar solvation energies. E_disp represents the solute-solvent dispersion energy. *G* is the summation of all the above terms and Δ*G* is the relative free energy calculated with respect to the parallel-stranded topology in the same force-field. All the values were rounded-off to the nearest whole numbers.

[b] The simulations were carried with the full GQ in 0.15 M excess NaCl. Only the GSs were used for MM-PBSA calculations. The 3'-terminal hydrogen was removed from parallel-stranded and antiparallel-basket GQ for MM-PBSA calculations to maintain equal number of atoms in all the GSs.

Table S3. MM-PBSA-based free energies[a] (kcal/mol) of the GSs of Htel topologies[b] in the simulations carried out in 0.15 M excess NaCl

GS-Topology	MM_ele	MM_vdw	MM_int	PB_sur	E_disp	PB_cal	*G*	Δ*G*
bsc0								
Parallel-stranded	-1993	-105	552	25	-233	-999	-2753	0
Antiparallel basket	-1957	-99	537	25	-234	-1027	-2755	-2
Hybrid-1	-2033	-100	546	25	-232	-968	-2762	-9
Hybrid-2	-2017	-101	539	25	-232	-985	-2771	-18
Antiparallel (2+2)	-1974	-102	526	25	-230	-1020	-2775	-22
bsc0χ_{OL4}								
Parallel-stranded	-1995	-104	550	25	-233	-998	-2755	0
Antiparallel basket	-1961	-101	540	25	-233	-1029	-2759	-4
Hybrid-1	-2013	-101	542	25	-232	-988	-2767	-12
Hybrid-2	-2022	-101	541	25	-231	-982	-2770	-15
Antiparallel (2+2)	-1978	-101	529	25	-232	-1020	-2777	-22
bsc0$\chi_{OL4}\varepsilon\zeta_{OL1}$								
Parallel-stranded	-2000	-101	552	25	-233	-992	-2749	0
Antiparallel basket	-1960	-101	545	25	-233	-1025	-2749	0
Hybrid-1	-2031	-101	549	25	-233	-971	-2762	-13
Hybrid-2	-2010	-101	539	25	-231	-989	-2767	-18
Antiparallel (2+2)	-2009	-100	539	25	-232	-992	-2769	-20

[a] The individual terms in the Table are explained in the footnotes of Table S2.

[b] Simulations and MM-PBSA calculations were carried out on the GSs of Htel topologies.

Table S4. MM-PBSA-based free energies[a] (kcal/mol) of GSs of Htel topologies[b] in the simulations carried out in 0.15 M excess KCl

GS-Topology	MM_ele	MM_vdw	MM_int	PB_sur	E_disp	PB_cal	*G*	Δ*G*
bsc0								
Parallel-stranded	-1967	-100	553	26	-234	-995	-2717	0
Antiparallel basket	-1913	-99	540	25	-233	-1036	-2716	1
Hybrid-1	-1998	-97	542	25	-234	-974	-2736	-19
Hybrid-2	-1990	-96	539	25	-233	-983	-2738	-21
Antiparallel (2+2)	-1948	-98	527	25	-231	-1016	-2741	-24
bsc0χ_{OL4}								
Parallel-stranded	-1968	-100	551	26	-234	-993	-2718	0
Antiparallel basket	-1940	-99	545	25	-234	-1019	-2722	-4
Hybrid-1	-1997	-97	548	25	-235	-975	-2731	-13
Hybrid-2	-1969	-99	537	25	-234	-998	-2738	-20
Antiparallel (2+2)	-1949	-97	529	25	-233	-1016	-2741	-23
bsc0$\chi_{OL4}\varepsilon\zeta_{OL1}$								
Parallel-stranded	-1974	-97	554	26	-238	-987	-2716	0
Antiparallel basket	-1939	-99	546	25	-234	-1019	-2720	-4
Hybrid-1	-2003	-98	549	25	-235	-965	-2727	-11
Hybrid-2	-1975	-99	539	25	-233	-990	-2733	-17
Antiparallel (2+2)	-1954	-98	531	25	-232	-1009	-2737	-21

[a] The individual terms in the Table are explained in the footnotes of Table S2.

[b] Simulations and MM-PBSA calculations were carried out on the GSs of Htel topologies

Note that the overall trend of energy variation among the topologies in GSs is similar to that observed in the simulations carried out in Na^+ ions (Table 1 (simulations without the loops, *i.e.*, GSs only simulations) and Table S3).

Table S5. MM-GBSA-based free energies (kcal/mol) of the Htel topologies in the simulations carried out in 0.15 M excess NaCl

Topology	G^a	ΔG^a	G^b	ΔG^b
bsc0				
Parallel-stranded	-2721	0	-2451	0
Antiparallel-basket	-2717	4	-2447	4
Hybrid-1	-2715	6	-2452	-1
Hybrid-2	-2715	6	-2459	-8
Antiparallel (2+2)	-2725	-4	-2466	-15
bsc0χ_{OL4}				
Parallel-stranded	-2720	0	-2452	0
Antiparallel-basket	-2716	4	-2449	2
Hybrid-1	-2718	2	-2457	-5
Hybrid-2	-2705	15	-2458	-6
Antiparallel (2+2)	-2726	-6	-2463	-11
bsc0$\chi_{OL4}\varepsilon\zeta_{OL1}$				
Parallel-stranded	-2721	0	-2447	0
Antiparallel-basket	-2719	2	-2441	6
Hybrid-1	-2718	3	-2452	-5
Hybrid-2	-2717	4	-2459	-12
Antiparallel (2+2)	-2726	-5	-2460	-13

.

[a] Simulations carried out with full GQ and subsequent MM-GBSA with GSs

[b] Simulations and MM-GBSA calculations carried out with the GSs only

G represents the energy of the topology while ΔG represents relative free energy with respect to parallel-stranded GQ in the same force-field**.**

Table S6. Relative free energies (kcal/mol) of Htel topologies in three independent sets of 100 ns long simulations with full GQ[a]

Topology	Relative free energy[b]	Relative free energy[c]	Relative free energy[d]
bsc0			
Parallel stranded	0	0	0
Antiparallel basket	21	16	10
	Stem-loop interaction		
Hybrid-1	20	17	15
Hybrid-2	11	12	20
Antiparallel (2+2)	5	13	12
bsc0χ_{OL4}			
Parallel stranded	0	0	0
Antiparallel basket	15	14	13
Hybrid-1	18	12	18
Hybrid-2	23	17	18
Antiparallel (2+2)	8	23	7
		cation distance ~6 Å	
bsc0$\chi_{OL4}\varepsilon\zeta_{OL1}$			
Parallel stranded	0	0	0
Antiparallel basket	13	19	23
			Stem-loop interaction
Hybrid-1	19	16	14
Hybrid-2	16	10	15
Antiparallel (2+2)	4	3	3

[a] The relative free energy of the topologies showed significant variations even within the same force-field. In topologies showing a difference of ≥10 kcal/mol from the lowest of the three values in the same force-field, the probable reason for deviation is noted below the relative free energy of the respective simulation.

[b,c,d] Relative free energies calculated from three independent MD simulations carried out in 0.15 M excess NaCl. The simulations were carried out with the full GQ and subsequent MM-PBSA calculations were carried out only on GSs.

Table S7. MM-PBSA-based free energies[a] (kcal/mol) of the model GQs[b]

Model	MM_ele	MM_vdw	MM_int	PB_sur	E_disper	PB_cal	*G*	ΔG
bsc0								
0	-1380	-104	549	27	-250	-1935	-3093	0
1	-1406	-100	557	27	-255	-1917	-3094	-1
2	-1358	-108	547	27	-252	-1946	-3090	3
3	-1392	-99	553	27	-254	-1920	-3085	8
4	-1426	-100	557	27	-252	-1895	-3089	4
5	-1394	-95	562	27	-259	-1924	-3083	10
6	-1376	-99	559	27	-253	-1931	-3073	20
7	-1452	-99	561	27	-256	-1886	-3105	-12
bsc0χ_{OL4}								
0	-1424	-103	554	27	-252	-1900	-3098	0
1	-1477	-103	561	27	-254	-1862	-3108	-10
2	-1427	-105	563	27	-252	-1891	-3085	13
3	-1415	-102	552	27	-252	-1904	-3094	4
4	-1466	-99	561	27	-254	-1861	-3092	6
5	-1486	-95	565	27	-257	-1853	-3099	-1
6	-1433	-101	569	27	-253	-1889	-3080	18
7	-1491	-100	566	27	-255	-1854	-3107	-9
bsc0$\chi_{OL4}\varepsilon\zeta_{OL1}$								
0	-1399	-104	549	27	-250	-1919	-3096	0
1	-1484	-101	561	27	-253	-1849	-3099	-3
2	-1379	-110	549	27	-249	-1932	-3094	2
3	-1397	-106	556	27	-250	-1912	-3082	14
4	-1466	-101	563	27	-253	-1860	-3090	6
5	-1489	-100	572	27	-252	-1846	-3088	8
6	-1433	-101	568	27	-253	-1884	-3076	20
7	-1484	-102	555	27	-251	-1848	-3103	-7

[a] The individual terms in the Table are explained in the footnotes of the Table S2.

[b] Simulations were carried with the full GQs but only GSs were used for MM-PBSA calculations. The simulations were carried out in 0.15 M excess NaCl.

Table S8. MM-PBSA-based relative free energies[a] (kcal/mol) of the model GSs[b] compared with the predictions based on the data by Cang *et al.* [34]

GS	Observed number of 5'-hydrogen bonds[c] in the simulations	Expected number of 5'-hydrogen bonds[c]	Calculated relative free energy (without the loops)			Predicted relative free energy (without the loops)[34]
			bsc0	bsc0χ_{OL4}	bsc0$\chi_{OL4}\varepsilon\zeta_{OL1}$	
0	2	**2**	0	0	0	**0**
1	2	**4**	-5	-1	-6	**-4**
2	2	**2**	-2	14	4	**19**
3	0	**0**	*27*	23	15	**33**
4	0	**2**	12	*31*	11	**29**
5	1	**2**	3	2	-5	**5**
6	0	**0**	18	*48*	11	**33**
7	2	**4**	-8	-8	-12 (30 -70 ns)	**-4**

[a] The relative free energies of the GS were calculated with respect to GS **0** in the same force-field

[b] Simulations and MM-PBSA calculations were carried out with only the GSs of the models. The MM-PBSA calculations were carried out on 50-100 ns region of the trajectory, unless specified.

[c] 5'-OH - (G)N3 H-bonds at the 5'-end of the GSs

The relative free energies of unstable GS arrangements are shown in italics in the Table. The relative free energy values were rounded-off to the nearest whole numbers.

Table S9. MM-PBSA-based free energies[a] (kcal/mol) of the GSs[b] of the models

GS	MM_ele	MM_vdw	MM_int	PB_sur	E_disper	PB_cal	*G*	Δ*G*
bsc0								
GS 0	-1957	-99	537	25	-234	-1027	-2755	0
GS 1	-1977	-101	539	25	-233	-1013	-2760	-5
GS 2	-1956	-107	538	25	-232	-1025	-2757	-2
GS 3	-1905	-104	538	25	-230	-1052	-2728	27
GS 4	-1958	-106	548	25	-231	-1021	-2743	12
GS 5	-1982	-102	553	25	-234	-1012	-2752	3
GS 6	-1927	-103	552	26	-235	-1050	-2737	18
GS 7	-1984	-95	542	26	-236	-1016	-2763	-8
bsc0χ_{OL4}								
GS 0	-1961	-101	540	25	-233	-1029	-2759	0
GS 1	-1998	-98	545	25	-235	-999	-2760	-1
GS 2	-1970	-105	547	25	-230	-1012	-2745	14
GS 3	-1917	-104	542	26	-232	-1051	-2736	23
GS 4	-1914	-106	547	25	-229	-1051	-2728	31
GS 5	-1969	-101	546	25	-235	-1023	-2757	2
GS 6	-1921	-110	553	25	-226	-1032	-2711	48
GS 7	-1997	-99	544	25	-235	-1005	-2767	-8
bsc0$\chi_{OL4}\varepsilon\zeta_{OL1}$								
GS 0	-1960	-101	545	25	-233	-1025	-2749	0
GS 1	-1991	-98	542	25	-233	-1000	-2755	-6
GS 2	-1974	-102	547	25	-232	-1009	-2745	4
GS 3	-1925	-103	545	25	-232	-1044	-2734	15
GS 4	-1978	-102	553	25	-233	-1003	-2738	11
GS 5	-1968	-101	548	25	-235	-1023	-2754	-5
GS 6	-1946	-103	549	25	-233	-1030	-2738	11
GS 7	-2002	-99	546	25	-235	-996	-2761	-12

[a] The individual terms in the Table are explained in the footnotes of the Table S2.

[b] Simulations and MM-PBSA were carried out only on the GSs of Htel topologies. The simulations were carried out in 0.15 M excess NaCl.

Table S10. MM-GBSA-based free energies (kcal/mol) of the antiparallel GQ models

	bsc0		bsc0χ_{OL4}		bsc0$\chi_{OL4}\varepsilon\zeta_{OL1}$	
Model[a]	***G***	**Δ*G***	***G***	**Δ*G***	***G***	**Δ*G***
0	-2704	0	-2705	0	-2706	0
1	-2702	2	-2707	-2	-2704	2
2	-2703	1	-2690	15	-2703	3
3	-2687	17	-2699	6	-2690	16
4	-2701	3	-2693	12	-2695	11
5	-2692	12	-2695	10	-2692	14
6	-2688	16	-2684	21	-2681	25
7	-2705	-1	-2704	1	-2708	-2
GS-Model[b]	***G***	**Δ*G***	***G***	**Δ*G***	***G***	**Δ*G***
GS **0**	-2447	0	-2449	0	-2441	0
GS **1**	-2453	-6	-2440	9	-2453	-12
GS **2**	-2451	-4	-2443	6	-2440	1
GS **3**	-2425	22	-2440	9	-2436	5
GS **4**	-2441	6	-2430	19	-2437	4
GS **5**	-2443	4	-2447	2	-2444	-3
GS **6**	-2453	-6	-2430	19	-2437	4
GS **7**	-2449	-2	-2451	-2	-2450	-9

[a] Simulations were carried out with complete GQs and subsequent MM-GBSA calculations were carried out only with the GSs.

[b] Simulations and MM-GBSA calculations were carried out only with the GSs of the models.

G represents the energy of the model while Δ*G* represent relative free energy with respect to model **0.** The simulations were carried out in 0.15 M excess NaCl.